Downlink Multiuser Superposition Using QPSK and 256-QAM in Mobile Communication Systems

Koki Senda and Hiroyuki Otsuka
Graduate School of Engineering, Kogakuin University,
1-24-2, Shinjuku-ku, Tokyo, 163-8677 Japan
Email: cm18023@ns.kogakuin.ac.jp

***Abstract*—Non-orthogonal multiple access (NOMA) is a potential candidate for the 5th-generation mobile systems (5G). In NOMA, two types of modulation signals are superposed for two different user equipment (UEs) in the power domain. The use of higher-order modulation such as 256-QAM is an also important technique under consideration for 5G. In this paper, we propose superposed modulation using QPSK and 256-QAM for downlink NOMA, and demonstrate the performance by link-level simulation under static propagation condition. The BER performance is investigated for the "superposed QPSK and 256-QAM" transmission as parameters of power allocation sets. From these results, we clarify the requirements for paired NOMA UEs when the superposed QPSK and 256-QAM is used in downlink NOMA.**

Keywords—Mobile communication, NOMA, Superposed modulation, 256-QAM, Power allocation

I. INTRODUCTION

5th-generation mobile systems (5G) need to provide much higher data rates, and much greater user throughput under higher connectivity density. 5G is also required to increase the system capacity and to realize much lower latency for a real time service [1]-[3].

Non-orthogonal multiple access (NOMA) has been considered for enhancing system performance, which can improve the spectrum efficiency towards 5G [4]-[9]. In the 3rd Generation Partnership Project (3GPP), NOMA for a paired user equipment (UEs) has been discussed to mainly implement in the downlink, i.e., the paired NOMA UEs (2 NOMA users) can share a same spectrum simultaneously. In the downlink, a superposed modulation and coding are applied to the paired NOMA UEs at the evolved Node B (eNB) transmitter.

In general, relatively higher transmission power is used for far UE with poor channel conditions. On the other hand, lower power transmission power is used for near UE with good channel conditions. In this case, it will be very important to decide the power allocation ratio for the paired NOMA UEs, as well as a scheduling methodology. From the modulation schemes perspective, at this stage, the superposed modulation has been discussed up to 64-quadrature amplitude modulation (QAM) on quadrature phase shift keying (QPSK) signals.

In order to improve data rates, a straightforward means is the use of higher-order modulation, which can increase the data rate within a given bandwidth. In Long Term Evolution (LTE) and LTE-Advanced mobile systems, QPSK, 16-QAM, and 64-QAM are being used for the symbol modulation of orthogonal frequency division multiplexing (OFDM).

In 5G, a modulation and coding scheme (MCS) will be used as well as 4G, in which the modulation scheme and related coding rate are adaptively chosen depending on the channel quality between eNB and UE. Thus far, the maximum modulation order is 64-QAM in the MCS. Recently, 256-QAM entry has been discussed mainly in the 3GPP, although 256-QAM application areas and/or conditions are very limited [10]-[13]. The reason is that the higher-order modulation scheme is at the cost of robustness to noise and interference.

Previously in [14]-[18], we proposed a OFDM-based 256-, 1024-, and 4096-QAM and demonstrated the fundamental transmission performance. The research motivation for the use of much-higher modulation is that a heterogeneous network (HetNet) and small cell enhancement (SCE) have been developed to potentially increase system capacity. Typical HetNets can cope with the increasing number of UEs in which small cells and/or pico cells are added to the existing macro cells. Both cell radius (pico cell in HetNet and small cell in SCE) will be short; therefore, it is expected that such a small cell environment could mitigate the fading impact.

Furthermore, three-dimensional (3D) beamforming has been also considered for enhancing system performance, which can adapt the antenna beam individually for each UE in the elevation domain. The 3D beamforming can promise to potentially increase the received signal-to-interference plus noise ratio (SINR) while directing less interference to adjacent cells/sectors and other UEs [19], [20]. Accordingly, the use of HetNet, SCE, and 3D beamforming and so on enhances the introduction of a higher-order modulation scheme, since these technologies can increase the received SINR.

Motivated by this observation, in this paper, we propose a superposed modulation using QPSK and 256-QAM in NOMA, and demonstrate the fundamental transmission performance such as BER as parameters of the power allocation sets.

The transmission model of the downlink multiuser superposition using QPSK and 256-QAM and the computer simulation conditions are described in Section II. In Section III, we present the BER performance versus received E_b/N_0 under additive white Gaussian noise (AWGN) environment. Finally, conclusions are summarized in Section IV.

II. Transmission Model And Simulation Conditions

Figure 1 illustrates a downlink NOMA scenario with one eNB and one paired UEs (near UE1 and far UE2). In typical case, eNB forms NOMA beamforming for paired UEs because the paired UEs are in the same direction when viewed from the eNB. Thus, near UE1 and far UE2 belong to same cluster as shown in Fig.1. The eNB transmits a superposed modulation signal simultaneously to both near UE1 and far UE2 with same frequency resource. The modulation scheme for far UE2 is always QPSK, and the transmission power for far UE2 is always higher than that for near UE1. The modulation scheme for near UE1 is determined using the channel state information (CSI) between near UE1 and eNB.

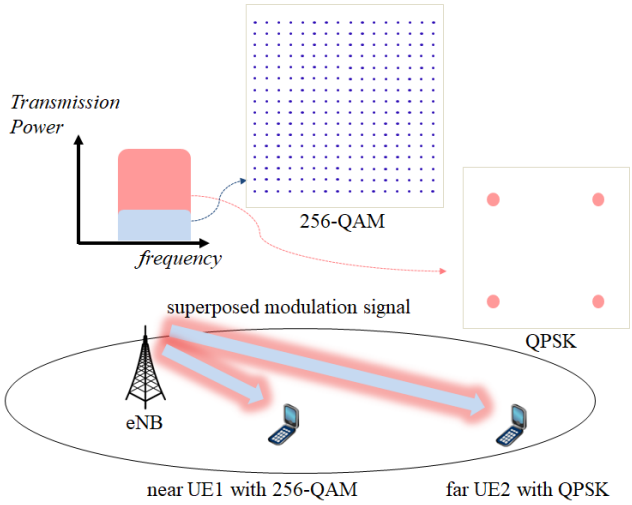

Fig. 1. Superposed modulation using QPSK and 256-QAM in downlink NOMA.

In NOMA, eNB can dynamically control the user throughput of each UE and optimize the system capacity and user fairness by adjusting the power allocation ratio.

Figure 2 shows the power allocation ratio for superposed modulation using QPSK and 256-QAM on first quadrant NOMA signal constellation at eNB transmitter. Here, the power allocation for far UE2 is δ_{QPSK}, and the power allocation for near UE1 is $\Sigma\, i\, \delta_{256\text{-}QAM,\,i} / 256$.

Figure 3 shows a block diagram of the downlink transmission model for 2 NOMA UEs. The channel between the eNB and each UE's is modeled by a typical AWGN. The transmitter antenna and the receiver antenna for both eNB and 2 NOMA UEs are consisted of a single branch. At the transmitter side, the baseband signals are encoded by turbo coding. The encoded signals are mapped to QPSK for far UE2 or 256-QAM for near UE1.

The power allocation for near UE1 and far UE2 are called P1 ($=\Sigma\, i\, \delta_{256\text{-}QAM,\,i} / 256$) and P2 ($=\delta_{QPSK}$), respectively. The power allocation sets are used with a constraint of the total transmission power is fixed to 1. When the transmission power is allocated for near UE1 and far UE2 to 0.1 and 0.9, respectively, the power allocation set is represented by (0.1, 0.9). In this simulation, OFDM is not employed for simplicity.

On the receiver of near UE1, a successive interference canceller (SIC) is implemented to remove the signal for far UE2. It is assumed that the interference (signal for far UE2) is ideally removed in the simulation. The UE2 receiver is not equipped with SIC, because the interference (signal for near UE1) must be less than thermal noise. Each component signal is demodulated by QPSK or 256-QAM demodulator. Each original baseband signals are detected after each Turbo decoder.

The main simulation parameters are summarized in Table I. QAM signals are mapped by the rule of Gray-code. The turbo coding scheme employs two identical convolutional encoders and one internal interleaver. The coding rate is fixed to 1/3. The soft decision of Viterbi decoding is used in the Turbo decoder.

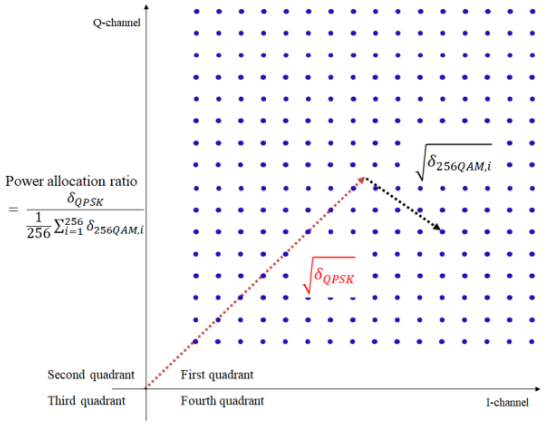

Fig. 2. Power allocation ratio for superposed modulation using QPSK and 256-QAM on first quadrant NOMA signal constellation.

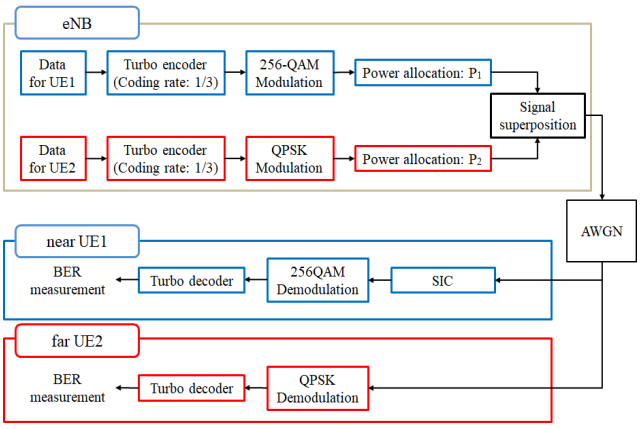

Fig. 3. Simulation block diagram of the downlink NOMA.

TABLE I. PRIMARY SIMULATION PARAMETERS

Parameter	*Assumption*
Modulation scheme	256-QAM for near UE1
	QPSK for far UE2
Power allocation sets (P1 for UE1, P2 for UE2)	(P1, P2) = (0.2, 0.8), (0.1, 0.9)
Turbo encoder	Parallel concatenated convolutional coding Coding rate : 1/3
Turbo decoder	Number of decoding iterations : 6
SIC	Ideal SIC
Number of Tx/Rx antennas	1
Channel condition	AWGN channel

III. LINK-LEVEL SIMULATION RESULTS

Figures 4(a) and 4(b) illustrate the superposed signal constellations using QPSK and 256-QAM at the eNB transmitter side with the power allocation sets of (0.2, 0.8) and (0.1, 0.9), respectively. Thus, a minimum Euclidian distance in 256-QAM is decreased with the progress of the increase of the power allocation for far UE2. This phenomena makes 256-QAM more sensitive to noise and interference, i.e., higher received SNR or E_b/N_0 is required to meet a certain quality.

Figure 5 shows the BER for both QPSK at far UE2 and 256-QAM at near UE1 versus received E_b/N_0 with the coding rate of 1/3. In this paper, we assumed that the E_b/N_0 to meet a BER of 10^{-2} is benchmark. When the power allocation set is (0.2, 0.8), the required E_b/N_0 for QPSK to meet a BER of 10^{-2} and 10^{-4} is approximately 2.4 and 2.7 dB, respectively. The required E_b/N_0 for 256-QAM to meet a BER of 10^{-2} and 10^{-4} is approximately 13.2 and 13.4 dB, respectively. Compared with the performance under no superposed modulation, i.e., only 256-QAM transmission, the required E_b/N_0 increases to around 6 dB.

Figure 6 shows the BER for the power allocation set of (0.1, 0.9). The required E_b/N_0 for QPSK to meet a BER of 10^{-2} and 10^{-4} is approximately 1.2 and 1.6 dB, respectively. The required E_b/N_0 for 256-QAM to meet a BER of 10^{-2} and 10^{-4} is approximately 16.2 and 16.4 dB, respectively. Compared with the performance under no superposed modulation, the required E_b/N_0 increases around 9.6 dB.

For QPSK, the required E_b/N_0 increases to around 2 and 1 dB compared with the performance under no superposed modulation, for the power allocation sets of (0.2, 0.8) and (0.1, 0.9), respectively.

Figure 7 shows the relation between required E_b/N_0 to meet a BER of 10^{-2} and power allocation P1 (power allocation sets) for both QPSK and 256-QAM. When the power allocation P1 for far UE2 is decreased, the required E_b/N_0 is increased, although the required E_b/N_0 for near UE1 with 256-QAM is increased. If the E_b/N_0 degradation is allowed up to approximately 3 dB for far UE2 with QPSK, the power allocation for near UE1 with 256-QAM can be increased up to 0.25, i.e., the power allocation set of (0.25, 0.75) is tolerable.

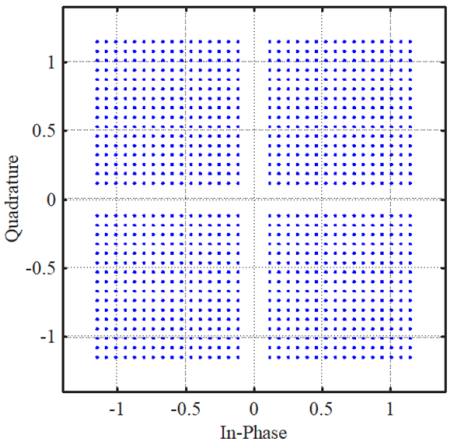

(a) Power allocation set of (0.2, 0.8)

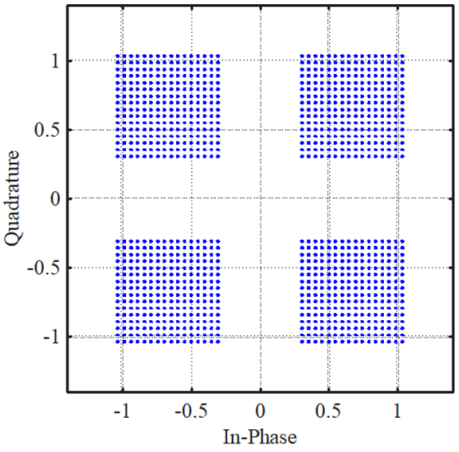

(b) Power allocation set of (0.1, 0.9)

Fig. 4. QPSK + 256-QAM NOMA signal constellation.

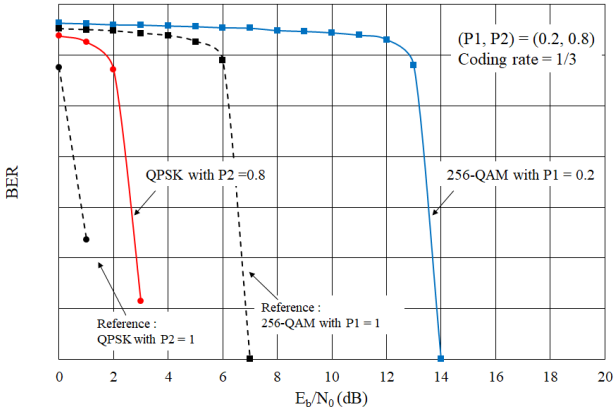

Fig. 5. BER performance of UE1 and UE2 with the power allocation set of (0.2, 0.8).

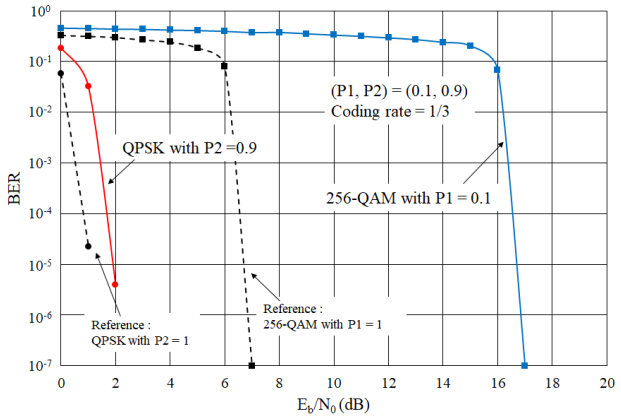

Fig. 6. BER performance of UE1 and UE2 with the power allocation set of (0.1, 0.9).

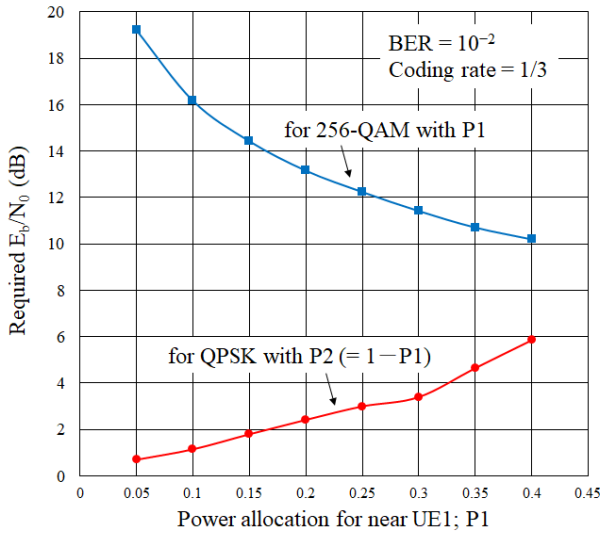

Fig. 7. Required E_b/N_0 for both UE1 (256-QAM with P1) and UE2 (QPSK with P2) to meet to meet a BER of 10^{-2} versus power allocation P1.

IV. Conclusion

This paper proposed multiuser superposed modulation using QPSK and 256-QAM for downlink NOMA, and presented the transmission performance such as BER as parameters of the power allocation sets by link-level simulations. When the transmission power is allocated to 0.1 for near UE with 256-QAM, i.e., the power allocation set of (0.1, 0.9) is used, the required E_b/N_0 for QPSK and 256-QAM to meet a BER of 10^{-2} is approximately 1.2 dB, and 16.2 dB, respectively. It is also clarified that if the E_b/N_0 degradation is allowed up to 3 dB for far UE2 with QPSK, the power allocation for near UE1 with 256-QAM can be increased up to 0.25, i.e., the power allocation set of (0.25, 0.75) is tolerable.

References

[1] J. G. Andrews, S. Buzzi, W. Choi, S. V. Hanly, A. Lozano, A. C. K. Soong, and J. C. Zhang, "What will 5G be ?," *IEEE Select. Area Commun.*, vol. 32, no. 6, pp. 1065-1082, June 2014.

[2] D. Soldani and A. Manzalini, "Horizon 2020 and beyond; On the 5G operating system for a truly digital society," *IEEE Vehicular Tech. Mag.*, vol. 10, no. 1, pp. 32-42, March 2015.

[3] 3GPP, News; "3GPP system standards heading into the 5G era," http://www.3gpp.org/news-events/3gpp-news/1614-sa_5g, 2014.

[4] Y. Saito, Y. Kishiyama, A. Benjebbour, T. Nakamura, A. Li, and K. Higuchi, "Non-orthogonal multiple access (NOMA) for future radio access," *in Proc.* VTC2013-Fall, pp.1-5, Sept. 2013.

[5] B. Kim, S. Lim, H. Kim, S. Suh, J. Kwun, S. Choi, C. Lee, S. Lee, and D. Hong, "Non-orthogonal multiple access in a downlink multiuser beamforming system," *in Proc.* MILCOM2013, pp. 1278–1283, Nov. 2013.

[6] 3GPP, TSG RAN WG1 Meeting #82, NTT DOCOMO, "System-level evaluation results for downlink multiuser superposition schemes," Aug. 2015.

[7] P. A. Hoeher and T. Wo, "Superposition modulation: Myths and facts," *IEEE Commun. Mag.*, vol. 49, no. 12, pp. 110-116, Dec. 2011.

[8] Z. Yang, Z. Ding, P. Fan, and N. Al-Dhahir, "A general power allocation scheme to guarantee quality of service in downlink and uplink NMA systems," *IEEE Trans. Wireless Commun.*, vol. 15, no. 11, pp. 7244-7257, Nov. 2016.

[9] E. Carmona Cejudo, H. Zhu, and O. Alluhaibu, "On the power allocation and constellation selection in downlink NOMA," *in Proc.* VTC2017-Fall, Sept. 2017.

[10] Q. Mu, L. Liu, L. Chen and Y. Jiang, "CQI table design to support 256 QAM in small cell environment," *in Proc.* WCSP2013, pp.1-5, Oct. 2013.

[11] 3GPP, R1-130341, Hitachi Ltd., "Views on 256QAM for small cell enhancement," emph RAN1 72 meeting, Feb. 2013.

[12] S. O. Ebassiouny and A. Ibrahim, "Link level performance evaluation of higher order modulation in small cells," *in Proc.* IWCMC2014, pp.850-855, Aug. 2014.

[13] J. Mao. M. A. Abdullahi, and A. Cao, "A low complexity 256QAM soft demapper for 5G mobile system," in Proc. EuCNC2016, June 2016.

[14] M. Iwamoto, S. Matsuoka, H. Iwasaki, and H. Otsuka, "Transmission Performance of OFDM with 1024-QAM in the Presence of EVM Degradation," *in Proc.* APWiMob2014, PHY1-3, Aug. 2014.

[15] M. Nakamura and H. Otsuka, "New Entry of OFDM using 256- and 1024-QAM in MCS Operation," *in Proc.* APWCS2015, RS4-2, Aug. 2015.

[16] T. Ota, M. Nakamura and H. Otsuka, "Possibility for New Entries of 1024- and 4096-QAM in Mobile Communication Systems," *in Proc.* APWCS2016, C5-1, Aug. 2016.

[17] T. Ota, M. Nakamura and H. Otsuka, "Performance Evaluation of OFDM-based 256- and 1024-QAM in Multipath Fading Propagation Conditions," *in Proc.* ICUFN2017, 7B-5, Aug. 2017.

[18] R. Tian, T. Ota, and H. Otsuka, "Influence of Phase Error on OFDM-based 4096-QAM with Turbo Coding," *in Proc.* ICOIN2018, F1-5, Jan. 2018.

[19] W. Lee, S-R. Lee, H-B. Kong, and I. Lee, "3D beamforming designs for single user MISO systems," *in Proc.* GCOM2013, pp.3914-3919, Dec. 2013.

[20] Y. Song, X. Yun, S. Nagata, and L. Chen, "Investigation on Elevation Beamforming for Future LTE-Advanced," *in Proc.* ICC2013, Workshop Beyond LTE-A, pp.106-110, June 2013.